Journal of Engineering Research

Volume 6 | Issue 2 Article 2

2022

Assessment of Micropiled Rafts Performance under Pure Lateral Loading

Ahmed Elsawwaf

Assessment of Micropiled Rafts Performance Under Pure Lateral Loading

Ahmed Elsawwaf[1*], Ashraf Nazir[2], Waseim Azzam[2]

[1*]MSc Student, Structural Engineering Department, Faculty of Engineering, Tanta University
[2]Ph.D. Professor, Structural Engineering Department, Faculty of Engineering, Tanta University
Emails: ahmed.elsawwaf@f-eng.tanta.edu.eg

Abstract- A micropile is a small diameter "cast-in-situ" pile which was initially used to repair historic buildings. In this paper, a numerical analysis was conducted on the performance of micropiled rafts under pure lateral loading using the finite element modelling. The FEM was calibrated against full scale lateral and axial field tests. Numerous cases were analyzed to investigate the lateral performance of micropiled raft on soft clay soil underlain by a layer of dense sand. The factors that may affect its performance were considered such as: the micropiles spacing, the undrained shear strength and thickness of upper clayey soil layer. The lateral load response of the micropiled raft was assessed. Moreover, the variation of lateral load capacity of single free head micropile with the clay cohesion was evaluated. Then, the effect of the micropiles spacing on the group efficiency was studied. The group effect was found to be insignificant for spacing to diameter ratio larger than 2.31.

Keywords: ***Finite element, Group efficiency, lateral load capacity, Micropiled raft, Shear strength.***

I. INTRODUCTION

A micropile is a small diameter "cast-in-situ" pile. Micropiles were initially used to repair historic buildings damaged during World War II, which required installing micropiles by drilling through the existing foundation and filling the holes with cement grout and a steel bar (Lizzi 1982). Micropiles are currently used in two general applications: for structural support and less frequently as in-situ reinforcement. Structural support includes new foundations, underpinning of existing foundations, seismic retrofitting applications and earth retention. In-situ reinforcement is used for slope stabilization, earth retention, and ground strengthening and protection (FHWA 2005). Micropiles can be installed by pouring the grout under gravity (Type A) or by pouring pressurized grout (Type B, Type C and Type D). Micropiles installation methods contribute to the enhancement of the grout-ground bond strength along the shaft of a micropile. The concept of the micropiled raft is similar to the concept of the piled raft, which is a composite structure with three components: subsoil, raft, and piles. The underpinning of existing structures may be performed for many purposes:

- To prevent structural movement.
- To enhance load-bearing capacity of existing structures.
- To repair inadequate foundations.
- To raise settled foundations to their original elevation.
- To transfer loads to a deeper stratum.

Increased load-bearing capacity of an existing foundation may be required for several reasons. Additional vertical, lateral, or vibratory loads may be applied to the foundation due to expansion of the existing structure, increased magnitude of applied loads, or the addition of vibrating machinery (FHWA 2005).

A. Background

Teerawut (2002) performed lateral load tests on vertical micropiles with different diameters installed in sand soil of different relative densities. The main observation was that the stiffness of the p-y curves increased as the pile diameter increased especially in dense sand. Richards and Rothbauer (2004) conducted lateral load tests on 20 vertical micropiles on eight different projects. Length-to-diameter ratios were greater than 20 in all micropiles which consisted of steel casing(s) filled with grout. Their diameters ranged from 197 mm to 381 mm. The grout unconfined compressive strength was 34.5 MPa and the yield strength of the steel casing was 552 MPa. The main observation was that the lateral load behavior is based on the soil type and shear strength in the upper 2 to 5 meters of the micropile. Long et al. (2004) performed lateral load tests on 10 micropiles that were 15.2 m long and reinforced with steel casings 244 mm outer diameter and 13.8 mm thick wall. The micropiles were installed for a seismic retrofit program of critical bridges. The ultimate lateral load varied between 53 kN and 123 kN. Abd Elaziz and El Naggar (2015) investigated the lateral performance of hollow bar reinforced micropiles through a field study and numerical analysis. Two monotonic and six cyclic lateral loading tests were performed on single micropiles in stiff to very stiff silty clay. The study tried to assess the impact of cased length of the hollow bar micropile on its lateral capacity.

There is a lack of research regarding the performance of the micropiled raft under pure lateral loading. Hence, an attempt has been taken in the present study to consider the possible effect of several parameters as well as the soil stratum in the lateral response of micropiled rafts.

B. Prime objectives of the study

The soil profile used in this study was soft clayey soil underlain by a layer of dense sand. An attempt has been taken to investigate the impacts of the undrained shear strength and thickness of upper clayey soil layer, and the micropiles spacing on micropiled rafts subjected to pure lateral loading. The prime objectives of the current study are to:

- Investigate the lateral load response of the micropiled raft.
- Evaluate the lateral load capacity of single micropile
- Discuss the impact of the micropiles spacing on the group effect

II. FINITE ELEMENT MODELLING

A. *Numerical model*

The 3D model used to carry out the analysis was developed using the computer code PLAXIS 3D. The validity of the FEA was checked by using the results of full-scale field loading tests that were obtained from (Kyung et al. 2017; Kyung and Lee 2018) and comparing them with those obtained from the FE analyses. A half of the micropiled raft foundation was modeled due to the symmetry to decrease the computation time. The horizontal side boundary was kept 3.2 B_r (where B_r is the raft width) and the vertical side boundary was kept 4.6 B_r as shown in Fig. 1. 3D 10-node tetrahedral elements were used to model the soil and micropiles while the raft foundation was modeled using 6-node triangular plate elements. The raft and micropiles were assumed to be linear elastic materials. The Mohr-Coulomb model was chosen for simulating the behavior of the soil. In PLAXIS 3D, an interface reduction factor, R_{int}, is used to model the interface element.

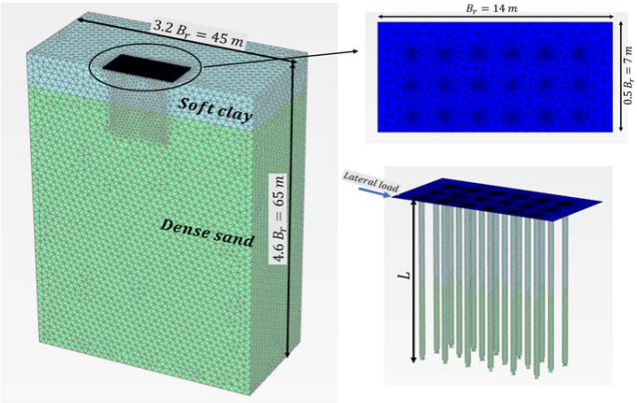

Fig. 1. 3D FEM used in the analysis and mesh pattern.

B. *Comparison and validation of the model*

The developed numerical model was validated in two stages. In the first stage, the results of full-scale field lateral loading tests of a single micropile Type A were compared with those obtained from the FE analysis. Then, in the second stage, the results of full-scale field axial loading tests of a single micropile Type C were compared with those obtained from the FE analysis.

B.1 Case -1: field lateral loading test of a single micropile Type A

The validation process was conducted by comparing the estimated load-deformation behavior with the measured one by Kyung and Lee (2018). The test site was located at Gongju city in Korea. Figure 2 introduces the depth profiles of SPT N and a detailed test configuration for the field load tests. Since the Type A gravity grouting technique was used in the micropile construction, R_{int} was assumed to be 0.7. Moreover, no preshearing of the soil was expected which would in turn cause no increase in the coefficient of lateral earth pressure (K_s).

All input parameters used in the FEM for both silty sand and the micropile are listed in Table 1. Figure 3 shows lateral load versus displacement behavior from numerical analysis compared to field test results obtained by Kyung and Lee (2018). With these values, a reasonable match with the full-scale field test results was achieved.

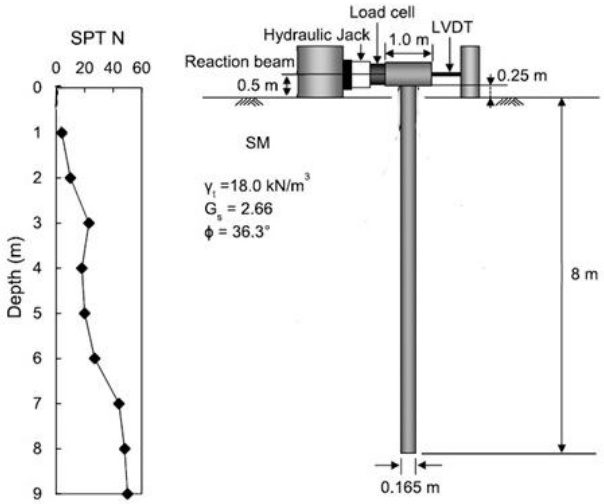

Fig. 2. Full-scale field load tests at Gongju site (Kyung and Lee 2018).

Table 1. Input parameters used in the FEM.

Parameter	Silty sand soil	Single micropile
Constitutive modelling	Mohr-Coulomb	Linear Elastic
Unit Weight (kN/m^3), γ_d	18	24
Angle of internal friction, Ø	36.3°	-
Dilation angle, ψ	6.3°	-
Average Modulus of Elasticity of micropile	-	52 GPa
Initial Modulus of Elasticity, E_o	1800 kPa	-
Incremental Modulus of Elasticity (kPa/m), E_{inc}	1600	-
Poisson's ratio, ν	0.3	0.15
Interface reduction factor, R_{int}	0.7	-

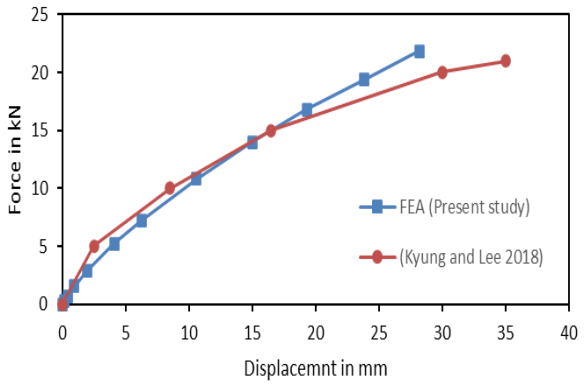

Fig. 3. 3D FEA calibration and verification results with full-scale field load tests of a single micropile of Type A (Kyung and Lee 2018).

B.2 Case -2: field axial loading test of a single micropile Type C

The validation process was conducted by comparing the estimated load-deformation behavior with the measured one by Kyung et al. (2017). The test site was located at Gochang city in Korea where layers of silty sands and clay were observed. Figure 4 presents the depth profiles of SPT N and a detailed test configuration for the field load tests. As shown in the figure, the top 1 m soil layer was silty sand. Low-plasticity clay existed between depths of 1 and 6 m with low SPT N, indicating soft and compressible conditions. A silty sand layer then existed below 6 m.

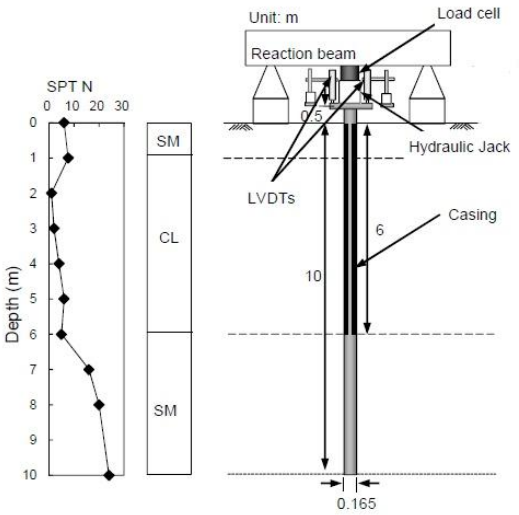

Fig. 4. Full-scale field load tests at Gochang site (Kyung et al. 2017).

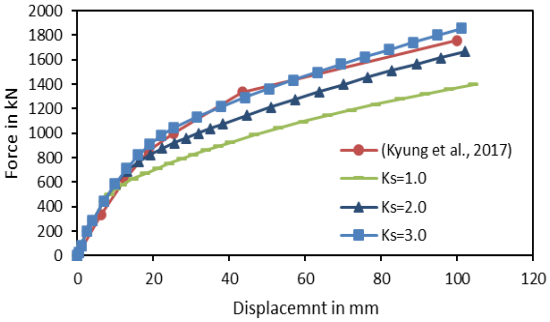

Fig. 5. 3D FEA calibration and verification results with full-scale field axial load tests of a single micropile of Type C (Kyung et al. 2017).

Since the Type C grouting technique was used in the micropile construction, R_{int} was assumed to be 0.95 (Alnuaim et al. 2016). Moreover, densification of the soil was expected which would in turn cause increase in the K_s value in the lower silty sand layer (uncased bond zone). Hence, a primary run of the PLAXIS program was performed to assign a K_s value that can be adopted to ensure that the micropile behavior is simulated in an accepted manner. Similar approach was used by Farouk (2009) to evaluate the optimum value in K_s.

Figure 5 shows the variation of the vertical load versus displacement behavior of a single micropile of Type C using different values of K_s for the lower silty sand layer. The studied values began from a value of 1.00. Then, the K_s value was increased in successive runs till there was an acceptable matching between the estimated results and the field test results at a K_s value of 3.00. All input parameters used in the FEM for the soil layers and the micropile are listed in Table 2.

C. *Model configuration and parametric study*

In the present study, a 14 m x 14 m x 0.8 m raft supported on 250 mm in diameter micropiles was used. A 6 x 6 micropile group was connected to the raft. The micropiles length was 13 m. The soil profile used was soft clay soil underlain by a layer of dense sand. Figure 6 depicts the model configuration, whereas Table 3 shows the input parameters of micropiles, and raft used in the FE analysis. The studied parameters include the undrained shear strength of upper clay soil layer (S_u), its thickness to micropile length ratio (t/L), and micropiles spacing to diameter ratio (s/d), as shown in Table 4.

Table 2. Input parameters used in the FEM.

Parameter	Upper silty sand	Clay	Lower silty sand	Single micropile
Constitutive modelling	Mohr-Coulomb	Mohr-Coulomb	Mohr-Coulomb	Linear Elastic
Unit Weight (kN/m^3), γ_d	17.58	18.77	17.83	24
Angle of internal friction, ∅	28.64°	0	33.52°	-
Dilation angle, ψ	0	0	3.52°	-
Cohesion, S	17.4 kPa	22.4 kPa	32.6	-
Average Modulus of Elasticity	5000 kPa	20000 kPa	20000 kPa	85 GPa
Poisson's ratio, ν	0.3	0.4	0.3	0.15
Interface reduction factor, R_{int}	0.70	0.70	0.95	-

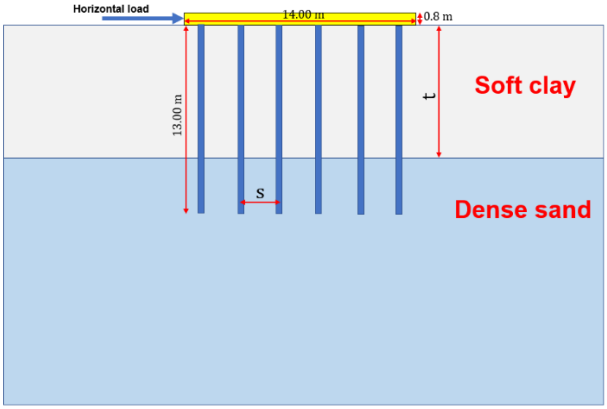

Fig. 6. Model configuration used in the FEA.

Table 3. Input parameters of micropiled raft used in FEM.

Parameter	Raft	Micropile
Constitutive modelling	Linear Elastic	Linear Elastic
Unit Weight (kN/m^3), γ_d	24	24
Modulus of Elasticity	$22 * 10^6$ kPa	$52 * 10^6$ kPa
Poisson's ratio, ν	0.15	0.15

Table 4. Parametric study.

Constant parameters	Variable parameter	Model
t/L = 0.54, s/d=8	S_u = 25,50,100,200 kPa	Micropiled raft
S_u = 25kPa, s/d=8	t/L = 0.25,0.38,0.54,0.75	Micropiled raft
S_u = 25kPa, t/L = 0.54	s/d=6,8,10	Micropiled raft
t/L = 0.54	S_u = 25,50,100,200 kPa	Single micropile

D. *Soil parameters*

The Mohr-Coulomb model was chosen for simulating the behavior of the soil in the FE analyses. The interface reduction value (R_{int}) was assumed 0.95 to simulate the rough surface condition for the micropiles of type C (Alnuaim et al. 2018; Kyung and Lee 2018). The validation process results of the FE model were utilized to choose the optimum value of K_s for sand and was taken 3.0. In case of the upper clay layer, K_s value was expected to be lower than that of sand and was assumed 1.4. Table 5 summarizes input parameters used in the FEM for different soil layers. The

clay elastic modulus was changed and correlated to the undrained cohesion using the relationship proposed by Bjerrum (1972).

$$E=(500 \text{ to } 1500)\ S_u \quad (1)$$

where: E = elastic modulus of clay; S_u = undrained shear strength of clay.

Table 5. Input parameters of soil layers used in FEM.

Parameter	Clay layer	Sand layer
Unit Weight (kN/m³), γ_d	17.5	20
Angle of internal friction, Ø	-	40°
Dilation angle, ψ	-	10°
Elastic modulus (kPa)	variable	60000
Poisson's ratio, ν	0.4	0.3
Lateral earth pressure coefficient, K_s	1.4	3.0
R_{int}	0.95	0.95

III. ANALYSIS OF RESULTS

A. *Evaluation of lateral response of micropiled raft*

Throughout the current study, the lateral load capacity was specified at 0.1d lateral displacement which is often used in practice

A.1 Effect of undrained shear strength of clay soil layer

The effect of clay undrained shear strength on the lateral response of micropiled raft systems was studied by changing the value of S_u and the corresponding value of E. The elastic modulus of clay was correlated to S_u value using Eq. 1 and was taken 20000 kPa, 40000 kPa, 60000 kPa, and 100000 kPa at S_u values of 25 kPa, 50 kPa, 100 kPa, and 200 kPa respectively. Figure 7 depicts the variation of lateral response of micropiled raft systems with different undrained shear strength values of the clay layer.

Figure 8 shows that the increase in S_u of the clay enhances the lateral load capacity but with a decreasing rate of increase. The maximum lateral load for $S_u = 200$ kPa reaches 3.22 times the maximum one corresponding to $S_u =$ 25 kPa.

A.2 Effect of thickness of soft clay layer

The effect of the thickness of the clay layer on the lateral response of micropiled raft systems was studied. The micropiles length was kept constant at 13.0 m while the clay thickness was changed. Figure 9 shows the variation of the lateral load capacity that was found to decrease with increasing the ratio of t/L. However, Fig. 10 demonstrates decrease in the rate of reduction in the lateral load capacity with increasing the thickness of soft clay layer. The percent decrease of lateral load capacity at t/L ratios of 0.38, 0.54 and 0.75 was found to be 5%, 8% and 9.5% respectively. The decrease in the lateral load capacity with increasing the soft clay thickness can be attributed to its low undrained shear strength and the decrease of the micropiles portion length embedded in the dense sand. Hence, the passive soil resistance in front of the micropiles decreases.

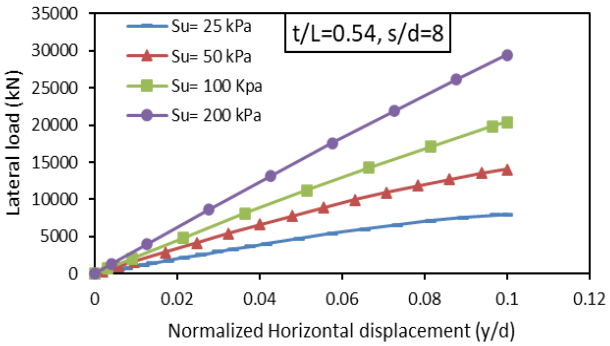

Fig. 7. Load displacement response of micropiled raft at different S_u values.

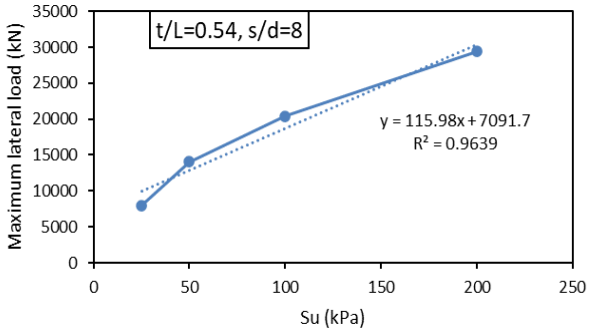

Fig. 8. Maximum lateral load taken by micropiled raft at different S_u values.

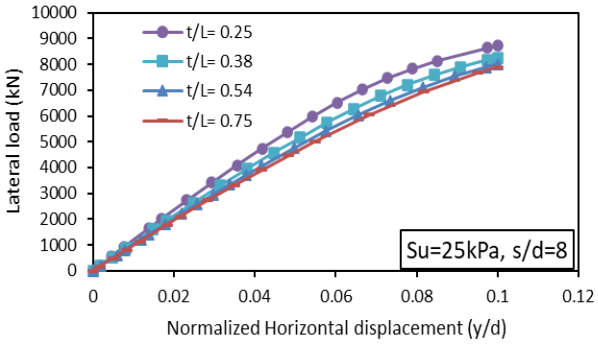

Fig. 9. Load settlement response of micropiled raft at different t/L values.

A.3 Effect of micropiles spacing to diameter ratio

Figure 11 presents the variation of lateral load response for the micropiled rafts at various s/d ratios. It can be observed that the lateral load capacity gets enhanced with increasing s/d ratio as shown in Fig. 12. There is almost 9% increase in the lateral load capacity, when the s/d is increased from 6 to 8, whereas the lateral load increased by 18% by increasing s/d from 6 to 10.

The reason for this behavior can be attributed to the 'micropile-micropile' interaction among the micropile group under the raft. When the spacing between the micropiles is increased, the overlapping between developed stress fields gets insignificant, causing larger resisting zone.

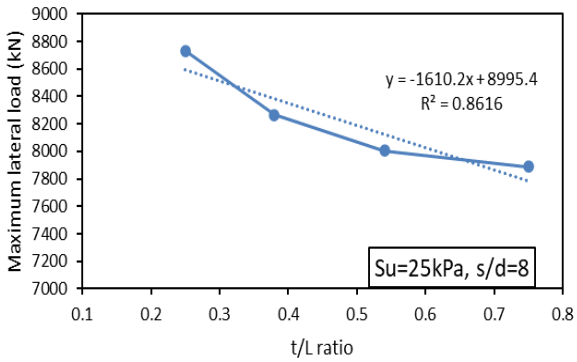

Fig. 10. Maximum lateral load taken by micropiled raft at different t/L values.

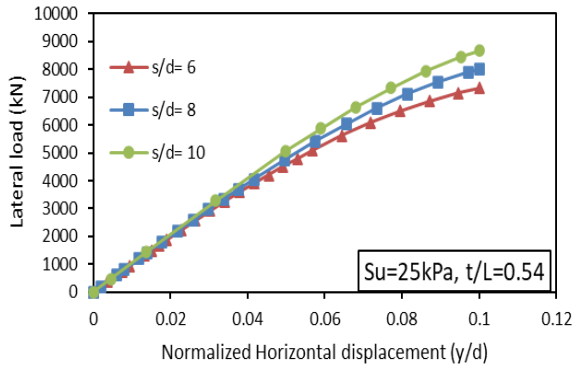

Fig. 11. Load settlement response of micropiled raft at different s/d values.

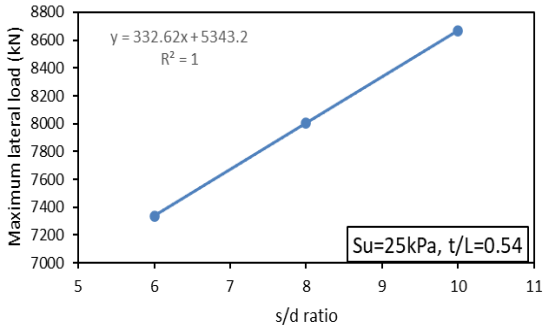

Fig. 12. Maximum lateral load taken by micropiled raft at different s/d values.

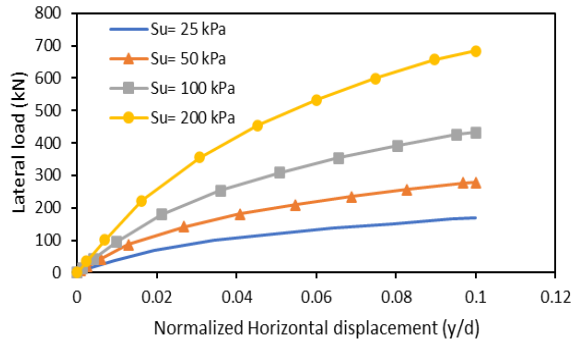

Fig. 13. Load settlement response of single free head micropile at different S_u values.

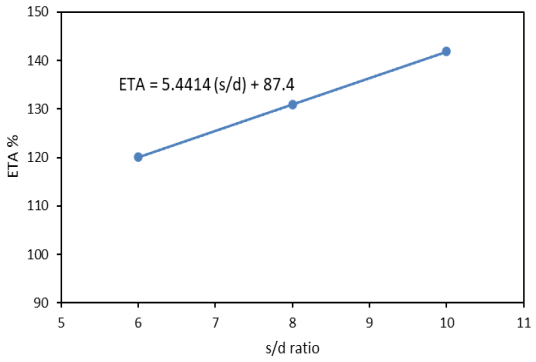

Fig. 14. Percent micropile group efficiency at various s/d ratios.

B. Evaluation of the lateral response of single free head micropile

B.1 Effect of undrained shear strength of clay soil layer

Figure 13 depicts the variation of lateral response of single free head micropile with different undrained shear strength values of the clay layer. The maximum lateral load for $S_u = 200$ kPa reaches 3.85 times the maximum one corresponding to $S_u = 25$ kPa.

C. Evaluation of the micropile group efficiency

In order to investigate the impact of the 36 micropiles spacing on the micropiles group effect, the group efficiency (ETA) was evaluated at various s/d ratios. The micropile group efficiency can be defined as

$$ETA = \frac{\text{lateral load capacity of micropiled raft}}{36 * \text{lateral load capacity of free head single micropile}} * 100 \quad (2)$$

Figure 14 presents the percent micropile group efficiency at various micropiles spacing to diameter ratios. The figure depicts that the ETA was greater than 100 % for the studied values of s/d. Furthermore, it is expected that the ETA will be less than 100 % if s/d gets less than 2.31. This finding is similar to that presented by Juran et al. (2008) who stated that the group effect gets significant when spacing to diameter ratio is smaller than 3.

IV. CONCLUSIONS

The main conclusions drawn from the numerical results are listed below:

- The lateral load carrying capacity of micropiled rafts increases with the increase of the upper clay undrained shear strength. The same trend is observed in the case of single free head micropiles.
- In case of soft upper clay layer, the lateral load capacity of micropiled rafts decreases with increasing the layer thickness.
- Considering that the number of installed micropiles is constant, the lateral load capacity of micropiled rafts increases with increasing spacing/diameter ratio.
- The percentage of the group efficiency was evaluated with various s/d ratios. It was found that the s/d ratio should be more than 2.31 to achieve group efficiency greater than 100 %. (The group effect gets insignificant)

REFRENCES

Abd Elaziz, Ahmed Yehia, and M. Hesham El Naggar. 2015. "Performance of Hollow Bar Micropiles under Monotonic and Cyclic Lateral Loads." *Journal of Geotechnical and Geoenvironmental Engineering* 141 (5). doi:10.1061/(asce)gt.1943-5606.0001279.

Alnuaim, A. M., M. H. El Naggar, and H. El Naggar. 2018. "Performance of Micropiled Rafts in Clay: Numerical Investigation." *Computers and Geotechnics* 99. doi:10.1016/j.compgeo.2018.02.020.

Alnuaim, Ahmed M., M. Hesham El Naggar, and Hany El Naggar. 2016. "Numerical Investigation of the Performance of Micropiled Rafts in Sand." *Computers and Geotechnics* 77. doi:10.1016/j.compgeo.2016.04.002.

Farouk, A. 2009. "Behavior of Micropiles under Vertical Tension and Compression Loads." In *Proceedings of the 17th International Conference on Soil Mechanics and Geotechnical Engineering: The Academia and Practice of Geotechnical Engineering*. Vol. 2. doi:10.3233/978-1-60750-031-5-1243.

FHWA. 2005. "Micropile Design and Construction Guidelines." *Handbook*, no. 132078.

Kyung, Doohyun, Garam Kim, Daehong Kim, and Junhwan Lee. 2017. "Vertical Load-Carrying Behavior and Design Models for Micropiles Considering Foundation Configuration Conditions." *Canadian Geotechnical Journal* 54 (2). doi:10.1139/cgj-2015-0472.

Kyung, Doohyun, and Junhwan Lee. 2018. "Interpretative Analysis of Lateral Load–Carrying Behavior and Design Model for Inclined Single and Group Micropiles." *Journal of Geotechnical and Geoenvironmental Engineering* 144 (1). doi:10.1061/(asce)gt.1943-5606.0001810.

Long, James, Massimo Maniaci, Glen Menezes, and Rory Ball. 2004. "Results of Lateral Load Tests on Micropiles." In . doi:10.1061/40713(2004)4.

Richards, Jr., Thomas D., and Mark J. Rothbauer. 2004. "Lateral Loads on Pin Piles (Micropiles)." In . doi:10.1061/40713(2004)7.